doi: 10.4149/gpb_2025023

HuR enhances the stability of FGF19 mRNA to suppress Kupffer cell activation and mitigate inflammation and fibrosis in non-alcoholic fatty liver disease

XiaoQing Mo[1,*], SiJun Zhou[2,*], XiaoGe Zhou[3] and Chun Huang[1]

[1] *Department of Endocrinology and Metabolism, Central People's Hospital of Zhanjiang, Zhanjiang City, Guangdong Province, China*
[2] *Department of Gastroenterology, Central People's Hospital of Zhanjiang, Zhanjiang City, Guangdong Province, China*
[3] *Department of Nutrition, Central People's Hospital of Zhanjiang, Zhanjiang City, Guangdong Province, China*

Abstract. This study explores how human antigen R (HuR) stabilizes fibroblast growth factor 19 (FGF19) mRNA, inhibiting Kupffer cell (KC) activation to reduce inflammation and fibrosis in non-alcoholic fatty liver disease (NAFLD). An animal model of NAFLD was established in mice by administering a high-fat diet (HFD). *In vitro* study utilized a lipopolysaccharide-induced immortalized mouse KC model. HuR expression markedly decreased in HFD-induced NAFLD liver tissue. Overexpression of HuR *via* adeno-associated virus (AAV) vectors mitigated key pathological features of NAFLD, including hepatic inflammation and fibrosis. Moreover, HuR overexpression suppressed KC activation in both *in vitro* and *in vivo* models. Mechanistically, HuR bound AU-rich elements in FGF19 mRNA, enhancing its stability. FGF19 overexpression similarly mitigated HFD-induced liver pathology. Conversely, FGF19 silencing reversed HuR's inhibition of KC activation and abrogated HuR's protection against liver inflammation and fibrosis. This research elucidates a novel mechanism underlying the interaction between HuR and FGF19 in mitigating the pathological progression of NAFLD, providing potential therapeutic targets for this prevalent liver disease.

Key words: HuR — NAFLD — Kupffer cells — FGF19 — Inflammation — Fibrosis

Introduction

Non-alcoholic fatty liver disease (NAFLD) is a condition mainly marked by widespread macrovesicular fat accumulation in the liver, occurring without alcohol intake or other obvious liver damage causes. The disease spectrum includes simple steatosis and non-alcoholic steatohepatitis (NASH), with potential progression to liver fibrosis, cirrhosis, and hepatocellular carcinoma (HCC) (Cotter and Rinella 2020; Abdelmalek 2021; Powell et al. 2021). With a prevalence of 25% among adults, NAFLD is now identified as the most prevalent chronic liver disease globally (Lazarus et al. 2022). Current evidence suggests that hepatic lipid metabolism dysregulation, inflammation, oxidative stress, and hepatocyte apoptosis are key contributors to disease onset (Loomba et al. 2021). The therapeutic objective in NAFLD management is to alleviate steatosis, prevent fibrosis, and mitigate inflammation, thereby delaying or halting disease progression. While numerous agents targeting lipid metabolism, inflammation, and fibrosis pathways are in clinical development, no pharmacological therapies have yet demonstrated definitive clinical efficacy (Makri et al. 2021; Paternostro and Trauner 2022; Rong et al. 2022).

During the course of NAFLD, approximately 20% of patient's progress to NASH, and more than 40% of NASH patients develop liver fibrosis (Xu et al. 2022). Preventing

* These authors contributed equally to this work.
Correspondence to: SiJun Zhou, Department of Gastroenterology, Central People's Hospital of Zhanjiang, No. 236 Yuanzhu Road, Chikan District, Zhanjiang City, Guangdong Province, 524045, China
E-mail: DR.zhou-1816@outlook.com

the progression of liver fibrosis is crucial to blocking the development of NAFLD-related cirrhosis and HCC (Friedman et al. 2018). Kupffer cells (KCs), the liver's resident macrophages, play a central role in hepatic inflammation, residing within the liver sinusoidal spaces (Li et al. 2017; Park et al. 2023). Liver injury is initiated by the activation of KCs, leading to the production of cytokines and chemokines that perpetuate the inflammatory response (Kolios et al. 2006). KCs are classified into M1 macrophages that promote inflammation and M2 macrophages that assist in tissue healing (Mosser and Edwards 2008; Dou et al. 2019). A key factor in fibrosis during NAFLD progression is the activation of M1 KCs. In opposition, the protective function against fibrosis in NAFLD is provided by the activation of M2 KCs (Wan et al. 2014; Kazankov et al. 2019). Therefore, inhibiting KC-mediated hepatic inflammation holds promise for ameliorating the transition from simple steatosis to NASH.

RNA-binding proteins (RBPs) are pivotal regulators of gene expression, modulating mRNA stability and translation efficiency through interactions with specific mRNA sequences (Corley et al. 2020). In the context of NAFLD, RBPs regulate various cellular processes, including transcription, alternative splicing, polyadenylation, mRNA stability, and subcellular localization. One such RBP, human antigen R (HuR) has been referred to as the "gatekeeper" of NAFLD (Subramanian et al. 2022; Xu et al. 2023). HuR, a member of the ELAV family of proteins, is conserved across both prokaryotes and eukaryotes (Schultz et al. 2020). Studies are increasingly pointing to HuR's role in liver lipid metabolism, where it serves as a defense against NAFLD-related fibrosis and HCC (Zhang et al. 2020; Tian et al. 2021; Wang et al. 2022). However, the influence of HuR on KC activation during NAFLD progression remains unexplored.

The regulation of target mRNA by HuR is largely dependent on its molecular structure. HuR has three RNA recognition motifs (RRMs) and a hinge region that enable it to bind to AU-rich elements in the 3′ untranslated regions (3′-UTR) of its target mRNAs. By stabilizing mRNA, this binding enhances its translation, with regulation happening at the transcriptional, post-transcriptional, and translational phases (Abdelmohsen and Gorospe 2010; Grammatikakis et al. 2017). Using bioinformatics tools such as ENCORI (https://rnasysu.com/encori/index.php) and ARED-PIUS (https://brp./ared), we predicted a potential interaction between HuR and fibroblast growth factor 19 (FGF19), identifying AU-rich regions within the 3′-UTR of FGF19. Based on these findings, we hypothesize that HuR may promote FGF19 mRNA stability by binding to its 3′-UTR, thereby inhibiting KC activation and attenuating inflammation and fibrosis in NAFLD. Our study aims to investigate the effects of HuR and FGF19 on NAFLD, elucidating the underlying molecular mechanisms by which these factors modulate inflammation and fibrosis.

Materials and Methods

Animal models and housing

Eight-week-old male C57BL/6J mice (18 ± 2 g) were procured from Beijing Vital River Laboratory Animal Technology Co., Ltd. (Beijing, China). Mice were housed in SPF-grade facilities at our institution, with 3–4 animals *per* cage. The setting was preserved at 22–26°C, humidity between 50–60%, and a cycle of 12 h of light and darkness. The mice were granted free access to both food and water during one week for acclimatization. Central People's Hospital of Zhanjiang (No. B2013380) Institutional Animal Care and Use Committee sanctioned every animal experiment.

Induction of NAFLD and experimental groups

NAFLD, along with associated inflammation and fibrosis, was induced in C57BL/6J mice through high-fat diet (HFD) feeding (Carmona-Hidalgo et al. 2021; Wei et al. 2023). Forty-eight mice were fed a HFD (60% kcal fat; Research Diets, NJ, USA) for 24 weeks, and were randomly assigned to six experimental groups (n = 8 *per* group): AAV9-HuR, AAV9-HuR-Ctrl, AAV9-FGF19, AAV9-FGF19-Ctrl, AAV9-HuR+sh-Ctrl, and AAV9-HuR+sh-FGF19. Adenoviral vectors targeting HuR (AAV9-HuR) and corresponding control (AAV9-HuR-Ctrl), FGF19-targeting shRNA or overexpression adenoviral vectors (AAV-sh-FGF19 or AAV9-FGF19), and their respective controls (AAV9-sh-Ctrl or AAV9-FGF19-Ctrl) were provided by Hanbio Tech (Shanghai, China). The thyroid-binding globulin promoter was employed to ensure hepatocyte-specific expression of the transgenes. Adenovirus was administered by tail vein injection (1×10^{11} genomic copies *per* mouse) at baseline and 12 weeks post-HFD feeding (Lin et al. 2023; Zhang et al. 2023). An additional group of eight mice was fed a normal chow diet (NCD; Research Diets) and served as controls.

Tissue collection and processing

Following completion of the experimental protocol, the mice were deprived of food for 12 h and then euthanized with an *intraperitoneal* injection of 1% sodium pentobarbital at a dose of 100 mg/kg. Blood was collected *via* retro-orbital plexus, immediately centrifuged, and serum was stored at 4°C for biochemical analysis. Liver tissues were excised, weighed, and liver index (liver weight/body weight, LW/BW) was calculated. A portion of the liver was fixed in 4% paraformaldehyde and embedded in paraffin for histological analysis, including Hematoxylin and Eosin (H&E) staining, Sirius Red staining, and immunofluorescence. Another portion was snap-frozen in liquid nitrogen for Oil Red O staining, while remaining tissues were homogenized for

biochemical assays. Additionally, a portion of liver tissue was stored at −80°C for quantitative real-time polymerase chain reaction (RT-qPCR) and Western blotting analyses.

Biochemical analysis

Serum alanine aminotransferase (ALT) and aspartate aminotransferase (AST) levels, as well as liver triglyceride (TG) and total cholesterol (TC) were measured using commercially available kits (Nanjing Jiancheng Bioengineering Institute, Nanjing, China).

Immunohistochemistry (IHC)

Paraffin-embedded liver tissue sections were subjected to standard deparaffinization and rehydration procedures, followed by endogenous peroxidase activity blocking with H_2O_2. Antigen retrieval was performed using microwave heating. To prevent nonspecific binding, sections were incubated with 10% normal goat serum for 30 min, then exposed to a primary antibody targeting HuR (1:500, ab200342, Abcam, Cambridge, UK) at room temperature for an hour. Following a rinse with phosphate-buffered saline (PBS), sections were treated with a secondary antibody (Proteintech, Rosemont, IL, USA) for 30 min. For signal detection, 3,3'-diaminobenzidine was utilized, and sections were counterstained with hematoxylin before mounting in neutral resin. HuR expression in liver tissues was examined under a light microscope (Olympus Optical Co., Ltd., Tokyo, Japan).

H&E staining

For H&E staining, liver tissue sections were deparaffinized and rehydrated through graded alcohols, followed by xylene clearing. Sections were stained with hematoxylin for 3–5 min, washed with deionized water, differentiated with 1% acid alcohol for 20 s, and blued with 1% ammonia for 30 s. Eosin staining was performed for 5 min, followed by thorough washing in deionized water. Sections were dehydrated and cleared in a graded alcohol series (75%, 90%, 95%, 100% ethanol), and then xylene-cleared. The slides were mounted for observation under an Olympus light microscope. The calculation of the NAFLD activity score involved assessing steatosis (0–3), lobular inflammation (0–3), and hepatocyte ballooning (0–2) (Kleiner et al. 2005).

Sirius red staining

Liver tissue paraffin sections were subjected to standard deparaffinization and rehydration procedures, followed by three washes with PBS for 5 min each. The slides were incubated with Sirius Red stain (Yisheng Biotechnology, Shanghai, China) at room temperature for 1 h, then washed with running water. Hematoxylin staining was performed for 30 s, followed by a 10-min rinse in running water. After dehydration through ethanol, the sections were cleared in xylene before being mounted. Liver fibrosis was observed using light microscopy (Olympus), and the extent of Sirius Red staining was quantitatively analyzed using ImageJ software (National Institutes of Health, USA).

Immunofluorescence staining

Tissue sections were deparaffinized and rehydrated as described previously, followed by washing in PBS. Antigen retrieval was performed twice, after which the slides were incubated in PBS for 15 min. Sections were incubated with normal serum to block non-specific binding, followed by treatment with the primary antibody against F4/80 (ab60343, Abcam) and an overnight incubation at 4°C in darkness. Sections were cleaned with PBS, and the appropriate fluorescence-conjugated secondary antibody (1:500, Invitrogen, CA, USA) was introduced and incubated at room temperature for 2 h. Nuclei were stained with DAPI for 15 min. Fluorescent images were acquired using an Olympus FV1200 confocal microscope system, and relative fluorescence intensity was quantified using ImageJ software.

Oil Red O staining

Frozen liver tissue sections (10 μm) were washed with PBS for 10 min, repeated three times, followed by 3 min of immersion in 60% isopropanol. The sections were stained with Oil Red O solution (Beijing Solarbio Science & Technology Co., Beijing, China) in the dark for 20 min, followed by a 1-min wash in 60% isopropanol to remove excess stain. After PBS washing, the sections were stained with hematoxylin for 2 min, followed by PBS washing and rebluing with ammonia solution for 2–3 s. Finally, the sections were mounted with glycerol-gelatin and examined under a light microscope. The Oil Red O-stained areas were quantified using ImageJ software.

Cell culture and transfection

Immortalized mouse KC line (ImKCs) was purchased from the cell bank of Procell Life Science & Technology Co. (Wuhan, China) and cultured in DMEM (Gibco, NY, USA) supplemented with 10% fetal bovine serum and 1% penicillin-streptomycin at 37°C in a 5% CO_2 incubator. For transfection, plasmids for overexpression of HuR (oe-HuR) and FGF19 (oe-FGF19), HuR shRNA, FGF19 shRNA, and the respective negative controls were obtained from GenePharma (Shanghai, China). The cells were cultured in six-well plates until they were 60% confluent, and then transfected with Lipofectamine 3000 (Invitrogen). Transfection ef-

ficiency was validated through RT-qPCR or Western blot. Subsequently, cells were treated with 500 ng/ml lipopolysaccharide (LPS, Sigma-Aldrich, MO, USA) for 24 h to establish a pro-inflammatory macrophage model (Wang et al. 2020; Tian et al. 2024).

Enzyme-linked immunosorbent assay (ELISA)

Cell culture supernatants and liver homogenates from the experimental mice were collected. The levels of TNF-α, IL-1β, IL-6, and IL-10 were measured using ELISA kits (R&D Systems, USA). According to the instructions provided by the manufacturer, all tests were completed.

Western blot analysis

Protein in liver tissues and cells was obtained utilizing a protein extraction kit (Thermo Fisher, USA). The BCA assay kit (Termo Fisher Scientifc Inc., MA, USA) was employed to measure protein levels. Each sample of protein (40 μg) underwent electrophoresis using 10% SDS-PAGE gels and was then moved onto polyvinylidene fluoride membranes through a semi-dry process at 0.8 mA/cm^2 for an hour at 4°C. Post an hour of blocking using 5% skimmed milk, the membranes underwent an overnight incubation at 4°C with primary antibodies targeting HuR (1:1000, ab200342, Abcam), FGF19 (1:1000, ab225942, Abcam), α-SMA (1:1000, ab5694, Abcam), Collagen I (1:1000, #72026, Cell Signaling Technologies, MA, USA), and β-actin (1:10000, 66009-1-Ig, Proteintech). The membranes underwent incubation with HRP-linked secondary antibodies (1:10000, #MR-R100/#MR-G100, Biotech, Beijing, China) for an hour at ambient temperature. Finally, the membrane was developed using a chemiluminescence substrate and the images were captured with a gel imaging system.

RT-qPCR

Total RNA was extracted from tissues and cells using TRIzol reagent (Invitrogen), and RNA concentration was measured using a Beckman UV spectrophotometer. cDNA was synthesized using a reverse transcription kit (K1621, Fermentas, USA) and stored at −20°C. Primer sequences (Table 1) were synthesized by GeneScript (Shanghai, China). qPCR was performed using the SYBR Green Premix Ex Taq (TaKaRa, Kusatsu, Japan) on an ABI 7500 Real-Time PCR System (Applied Biosystems Inc., MA, USA). PCR was conducted under these conditions: initially at 95°C for 5 min, then 35 cycles at 94°C for 45 s, 56°C for 45 s, and 72°C for 45 s. The $2^{-\Delta\Delta Ct}$ technique was employed to determine relative gene expression, using GAPDH as the internal control.

RNA immunoprecipitation (RIP) assay

RIP was performed using a RIP kit (Millipore, MA, USA). Briefly, cells were lysed with the complete RIP lysis buffer and incubated overnight at 4°C with beads pre-coated with anti-HuR or IgG antibodies. RNA was subsequently extracted using the RNeasy MinElute Cleanup Kit (Qiagen, Hilden, Germany), and the RNA enrichment levels on the specific probes were quantified by RT-qPCR.

Luciferase reporter assay

Plasmids containing the 5'UTR (Luc-FGF19-5'UTR), coding sequence (CDS) (Luc-FGF19-CDS), and 3'UTR (Luc-FGF19-3'UTR) of FGF19 were synthesized. Plasmid extraction was carried out using a standard plasmid extraction kit (Promega, WI, USA). Cells were co-transfected with the FGF19 plasmids and either the HuR overexpression plasmid or the corresponding negative control using Lipofectamine 3000 (Invitrogen). Forty-eight hours post-transfection, cells were harvested and lysed, and luciferase activity was measured using the Luciferase Assay System (BioVision, CA, USA).

mRNA stability assay

For mRNA stability assays, transfected KCs were cultured for 24 h and then treated with 4 μmol/l actinomycin D (Sigma-Aldrich). At 0, 3, 6, and 12 h post-treatment, cells were harvested, and RNA was extracted for RT-qPCR to analyze FGF19 mRNA levels.

Table 1. Primer sequences

Gene	Forward primer	Reverse primer
TNF-α	TACCCCTGCCTGAGAGCAAT	CCACTTGGTGGTTTGTGAGTG
IL-1β	GGGCCTCAAAGGAAAGAATC	TACCAGTTGGGGAACTCTGC
IL-6	TCTGCAAGAGACTTCCATCCA	AGTCTCCTCTCCGGACTTGT
IL-10	CTGGACAACATACTGCTAACCGACTC	ACTGGATCATTTCCGATAAGGCTTGG
HuR	TGGGCGAATCATCAACTCCA	CGGATAAAGGCAACCCCTCT
FGF19	CGGTCGCTCTGAAGACGATT	CCTCCGAGTAGCGAATCAGC
GAPDH	TGCACCACCAACTGCTTAG	GGATGCAGGGATGATGTTC

Statistical analysis

The analysis of the data was conducted utilizing GraphPad Prism 9 (GraphPad Software, CA, USA). The data presentation was in the form of mean ± standard deviation. The Student's *t*-test was utilized to compare two groups. To compare several groups, one-way ANOVA and Tukey's multiple comparisons test were employed. *p*-values below 0.05 were deemed to hold statistical significance.

Results

HuR expression is downregulated in NAFLD

To explore the role of HuR in NAFLD, we induced the disease in mice using a 24-week HFD. RT-qPCR, Western blot, and immunohistochemical analyses revealed a significant downregulation of HuR mRNA and protein expression in the liver of HFD-fed mice compared to controls on NCD (Fig. 1A–C). These findings indicate that HuR is underexpressed in NAFLD and suggest a potential inverse relationship between its expression and disease progression.

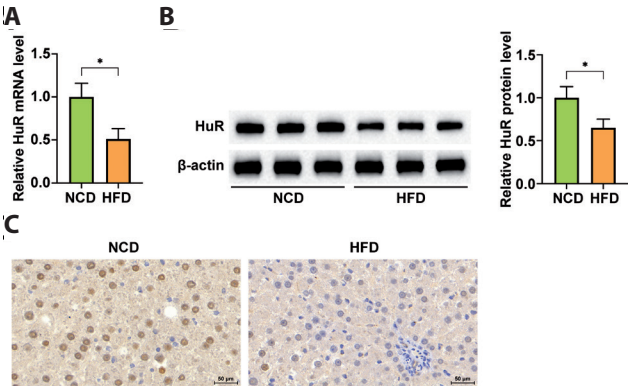

Figure 1. Downregulation of HuR expression in NAFLD. RT-qPCR analysis of HuR mRNA levels (**A**), Western blot analysis of HuR protein levels (**B**) and immunohistochemical staining for HuR protein expression (**C**) in liver tissues from a normal chow diet (NCD) and high-fat diet (HFD) mice. Data are presented as mean ± SD ($n = 8$); * $p < 0.05$.

HuR ameliorates hepatic fibrosis in NAFLD mice

To investigate the role of HuR in NAFLD, we employed AAV-mediated gene delivery to overexpress HuR in HFD-induced NAFLD mice. Overexpression of HuR in the liver was

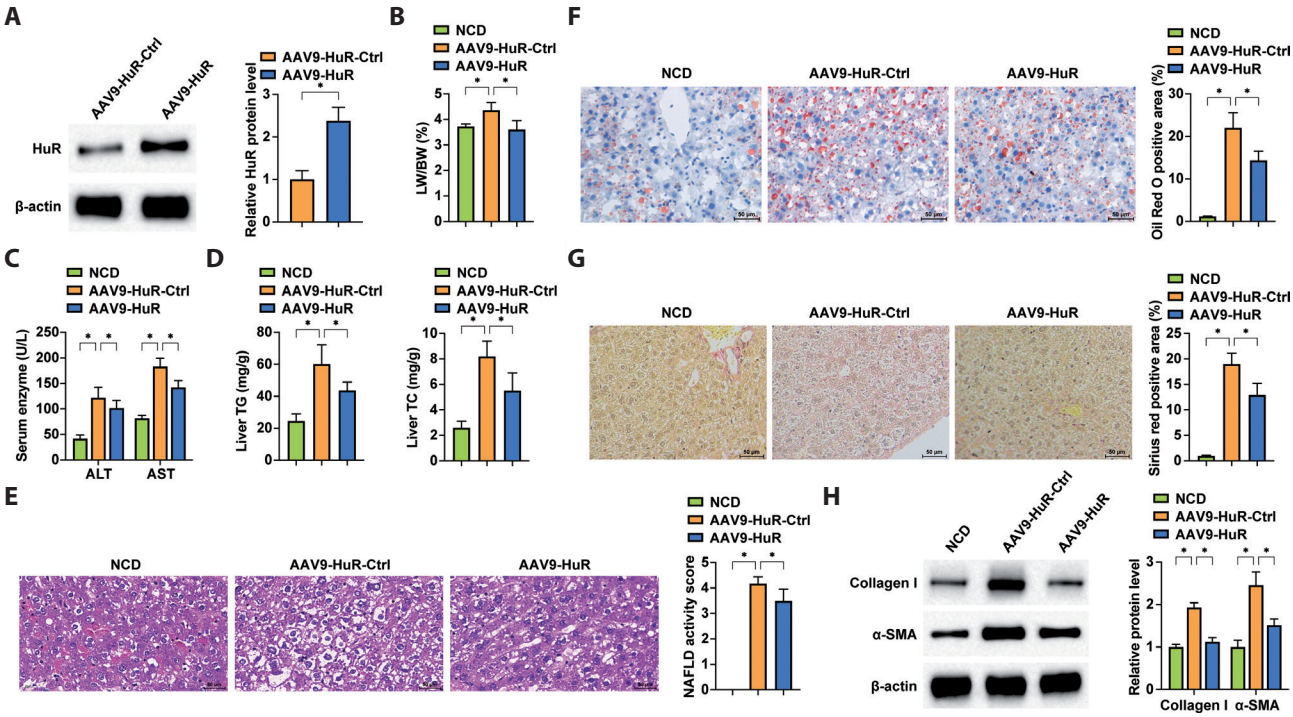

Figure 2. HuR alleviates liver fibrosis in NAFLD mice. **A.** Western blot analysis of HuR expression in liver tissues from different groups. **B.** LW/BW ratio in each group of mice. **C.** Serum AST and ALT activity levels. **D.** Hepatic TG and TC levels in liver tissues. **E.** Representative H&E staining images and NAS scores for liver tissues. **F.** Representative Oil Red O staining images and quantification of lipid accumulation in liver tissues. **G.** Sirius Red staining of liver tissues with corresponding fibrosis quantification. **H.** Western blot analysis of Collagen I and α-SMA protein levels in liver tissues. Data are presented as mean ± SD ($n = 8$); * $p < 0.05$.

confirmed by Western blotting (Fig. 2A). Functional assays revealed thatHuR overexpression led to a significant drop in LW/BW and helped reduce the elevated serum AST and ALT levels resulting from HFD (Fig. 2B,C), suggesting a protective effect against liver damage. Given that lipid metabolism is a hallmark of NAFLD, we next assessed hepatic TG and TC levels, key indicators of lipid accumulation. Compared to NCD mice, HFD-fed mice exhibited significantly elevated levels of both TG and TC in the liver, which were markedly reduced upon HuR overexpression (Fig. 2D). Histological examination further highlighted the pathological hallmarks of NAFLD in HFD mice, including lobular inflammation, steatosis, and hepatocyte ballooning. Notably, these features were notably alleviated by HuR overexpression (Fig. 2E). Oil Red O and Sirius Red staining revealed prominent lipid deposition and collagen accumulation in HFD-treated livers. However, HuR overexpression significantly attenuated both lipid accumulation and fibrosis (Fig. 2F,G). Additionally, Western blot analysis demonstrated reduced expression of key fibrosis markers, including Collagen I and α-SMA, in HuR-overexpressing livers (Fig. 2H). Collectively, these findings underscore the potential of HuR as a therapeutic target, suggesting that its upregulation can mitigate key pathological features of NAFLD, including hepatic injury, lipid accumulation, and fibrosis.

HuR mitigates KC activation and hepatic inflammation in NAFLD mice

In HFD-fed mice, immunofluorescence staining observed a significant increase in F4/80 expression, a well-established marker for KC infiltration. Remarkably, overexpression of HuR reduced this infiltration, suggesting a role for HuR in suppressing KC activation (Fig. 3A). The inflammatory response in macrophages is driven by both their recruitment and polarization. To assess the effects of HuR on macrophage polarization, we measured specific M1 and M2 markers in liver tissues using RT-qPCR and ELISA. Mice on a HFD showed significantly higher pro-inflammatory cytokines linked to M1, including TNF-α, IL-1β, and IL-6, while IL-10, an anti-inflammatory cytokine, was lowered. Notably, overexpression of HuR attenuated the inflammatory response, downregulating TNF-α, IL-1β, and IL-6 and restoring IL-10 levels (Fig. 3B,C). These findings underscore the pivotal role of HuR in mitigating KC activation and hepatic inflammation in NAFLD.

HuR suppresses KC activation in vitro

ImKCs, a specialized cell type with self-renewal capacity, reside within the hepatic microcirculatory spaces and are integral components of the mononuclear phagocyte system. These cells are considered potential therapeutic targets for NAFLD (Tran et al. 2020). To investigate the role of HuR in modulating KC activation *in vitro*, we utilized an LPS-induced inflammation model. Both RT-qPCR and Western blot analyses revealed a significant downregulation of HuR expression in the LPS-treated ImKCs (Fig. 4A,B). Transfection with HuR overexpression plasmid, along with the corresponding negative control, confirmed successful overexpression in LPS-treated ImKCs (Fig. 4C). Consistent with

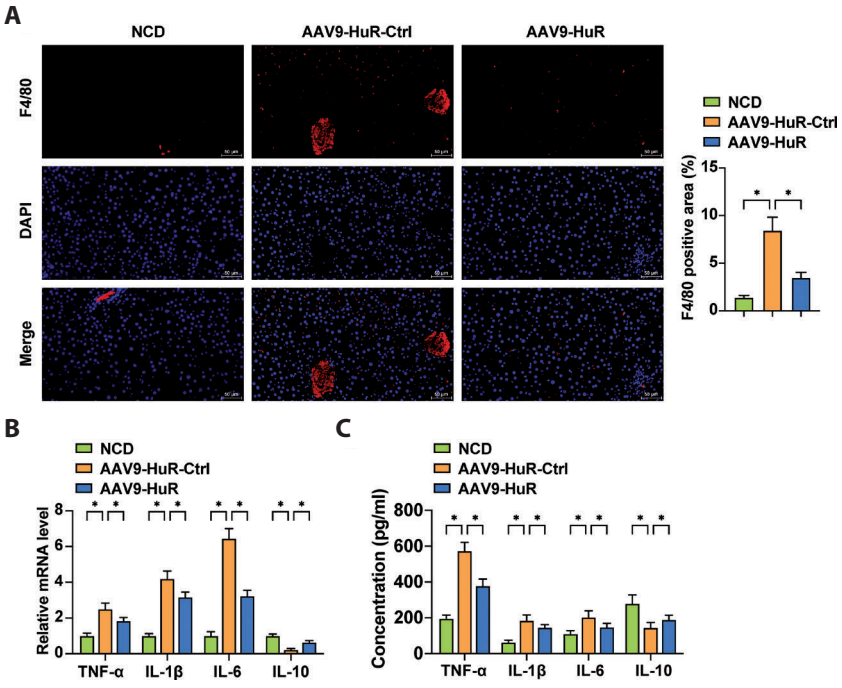

Figure 3. HuR suppresses Kupffer cell activation and hepatic inflammation in NAFLD mice. **A.** Immunofluorescence staining for F4/80 expression in liver tissues from different groups. RT-qPCR analysis (**B**) and ELISA measurement (**C**) of TNF-α, IL-1β, IL-6, and IL-10 mRNA levels in liver tissues. Data are presented as mean ± SD ($n = 8$); * $p < 0.05$.

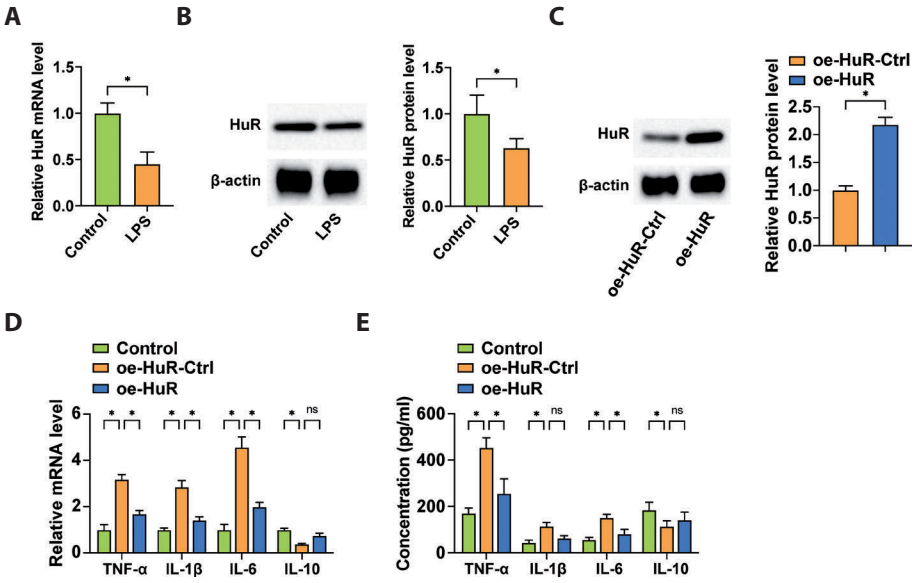

Figure 4. HuR inhibits Kupffer cell activation *in vitro*. RT-qPCR (**A**) and Western blot (**B**) analysis of HuR expression in LPS-treated cells. **C.** Western blot assessment of HuR protein expression in transfected cells. **D.** RT-qPCR analysis of TNF-α, IL-1β, IL-6, and IL-10 mRNA levels in cells. **E.** ELISA measurement of TNF-α, IL-1β, IL-6, and IL-10 levels in cell supernatants. All data are presented as the mean ± SD of at least 3 independent experiments; * $p < 0.05$.

in vivo findings, RT-qPCR and ELISA analyses showed that HuR overexpression reversed the LPS-induced increases in TNF-α, IL-1β, and IL-6 while promoting IL-10 (Fig. 4D,E). These results collectively demonstrate that overexpression of HuR counteracts LPS-induced inflammation and M1 polarization in KCs.

HuR promotes FGF19 mRNA stability

Computational predictions using ENCORI (https://rnasysu.com/encori/index.php) suggested a potential interaction between HuR and FGF19, which we confirmed through RNA immunoprecipitation (Fig. 5A). To assess the specificity of this interaction, we employed luciferase reporter assays. Overexpression of HuR markedly increased luciferase activity in cells transfected with the Luc-FGF19-3'UTR construct, supporting the notion that HuR directly influences FGF19 mRNA (Fig. 5B). Additionally, actinomycin D treatment revealed that HuR overexpression significantly delayed the decay of FGF19 mRNA, indicating enhanced mRNA stability. Conversely, silencing HuR accelerated the degradation of FGF19 mRNA (Fig. 5C). Western blotting further confirmed that HuR overexpression led to a corresponding increase in FGF19 protein levels, while HuR knockdown diminished its expression (Fig. 5D). The findings together indicate that HuR binds to the 3'-UTR of FGF19 mRNA, stabilizing it and increasing FGF19 expression post-transcriptionally.

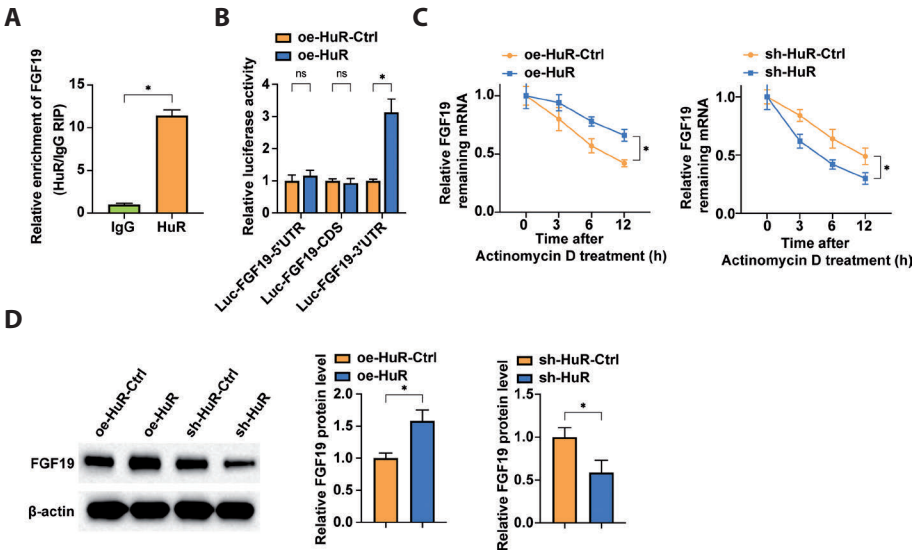

Figure 5. HuR promotes FGF19 mRNA stability. **A.** RIP assay confirming the interaction between HuR and FGF19 mRNA. **B.** Luciferase reporter assay showing the binding of HuR to the 3' UTR of FGF19. **C.** RT-qPCR analysis of FGF19 mRNA stability after actinomycin D treatment, with or without HuR overexpression or knockdown. **D.** Western blot analysis of FGF19 protein levels after HuR overexpression or knockdown. All data are presented as the mean ± SD of at least 3 independent experiments; * $p < 0.05$.

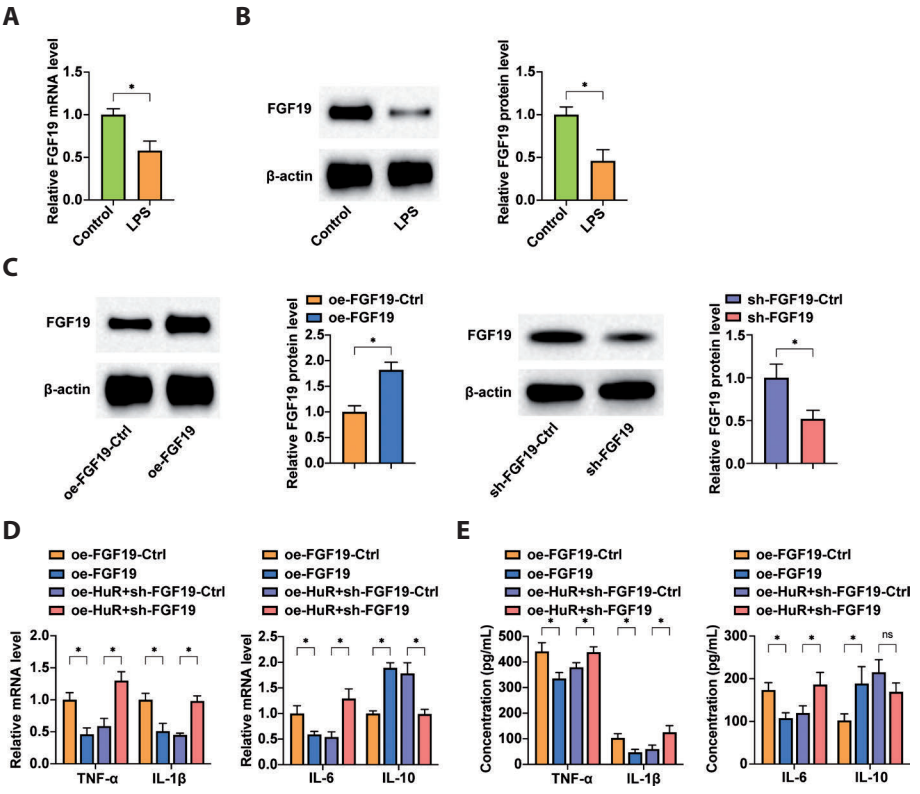

Figure 6. HuR suppresses Kupffer cell activation *via* FGF19. RT-qPCR (**A**) and Western blot (**B**) analysis of FGF19 expression in LPS-treated cells. **C.** Western blot detection of FGF19 protein expression in transfected cells. **D.** RT-qPCR analysis of TNF-α, IL-1β, IL-6, and IL-10 mRNA levels in cells. **E.** ELISA measurement of TNF-α, IL-1β, IL-6, and IL-10 levels in cell supernatants. All data are presented as the mean ± SD of at least 3 independent experiments; * $p < 0.05$.

HuR modulates KC activation through FGF19

In the LPS-induced ImKC inflammatory model, both RT-qPCR and Western blot analyses revealed a significant reduction in FGF19 expression (Fig. 6A,B). Overexpression of FGF19 in LPS-treated ImKCs, confirmed by Western blot (Fig. 6C), reversed the inflammatory response. Consistent with *in vivo* observations, overexpression of FGF19 decreased TNF-α, IL-1β, and IL-6, while increasing IL-10 (Fig. 6D,E). These findings indicate that FGF19 exerts a protective effect against LPS-induced KC activation, similar to HuR overexpression. To further elucidate the relationship between HuR and FGF19, we co-transfected ImKCs with oe-HuR and sh-FGF19 for a rescue experiment. Western blotting confirmed successful transfection (Fig. 6C). As expected, in the oe-HuR+sh-FGF19 group, the LPS-induced elevation of TNF-α, IL-1β, and IL-6 was restored, while IL-10 levels decreased. This suggests that HuR exerts its anti-inflammatory effects *via* FGF19, highlighting their cooperative role in modulating KC activation.

HuR ameliorates hepatic inflammation and fibrosis in NAFLD mice through FGF19

Both RT-qPCR and Western blot analysis revealed a marked reduction in FGF19 expression in the livers of HFD-fed mice compared to controls (Fig. 7A,B). To explore the role of FGF19 in mediating the effects of HuR, we employed AAV-mediated gene delivery to overexpress FGF19 in HFD-induced NAFLD mice. Overexpression of FGF19 in the liver was confirmed by Western blot (Fig. 7C). Strikingly, FGF19 overexpression significantly alleviated HFD-induced liver damage, as evidenced by a decrease in the LW/BW and reduced serum ALT and AST levels (Fig. 7D,E). Furthermore, elevating FGF19 reduced hepatic TG and TC levels (Fig. 7F). Histological examination revealed that FGF19 overexpression mitigated key pathological features of NAFLD, including lipid accumulation and fibrosis (Fig. 7G,H). Specifically, hepatic lipid deposits were diminished, and Collagen I and α-SMA levels were notably reduced (Fig. 7I,J). Moreover, FGF19 overexpression inhibited KC activation, as indicated by decreased F4/80 expression, and downregulated TNF-α, IL-1β, and IL-6, while enhancing cytokine IL-10 (Fig. 8A–C). These data strongly suggest that FGF19 overexpression counteracts liver inflammation and fibrosis in NAFLD, with effects resembling those observed following HuR upregulation.

An *in vivo* rescue experiment was performed to further verify FGF19's involvement in the protection mediated by HuR. Successful knockdown of FGF19 in the liver was confirmed *via* adenoviral-mediated transfection (Fig. 7C). Notably, FGF19 knockdown reversed the protective

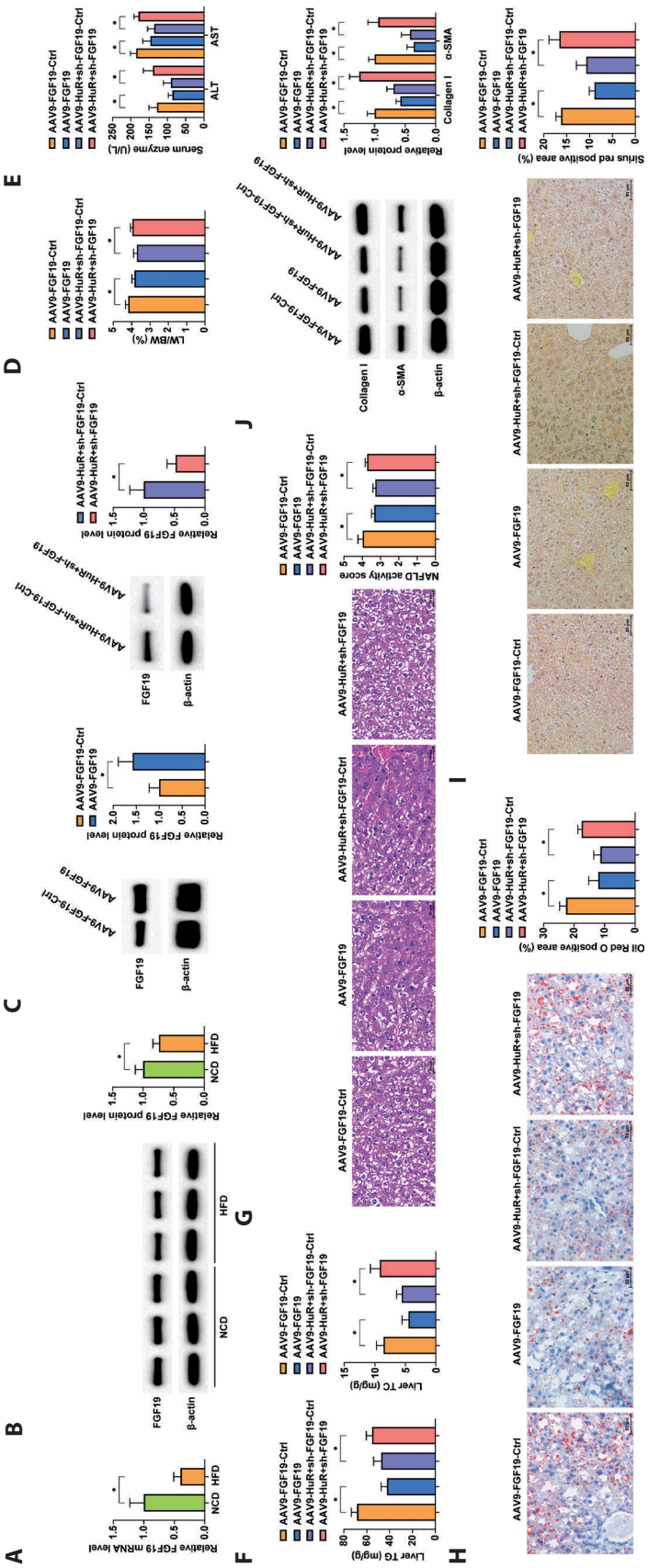

Figure 7. HuR ameliorates liver fibrosis in NAFLD mice *via* FGF19. RT-qPCR (**A**) and Western blot (**B**) analysis of FGF19 expression in liver tissues from different groups. **C.** Western blot assessment of FGF19 protein levels in liver tissues. **D.** LW/BW ratio in each group of mice. **E.** Serum AST and ALT activity levels. **F.** Hepatic TG and TC levels in liver tissues. **G.** Representative H&E staining images and NAS scores for liver tissues. **H.** Representative Oil Red O staining images and quantification of lipid accumulation in liver tissues. **I.** Sirius Red staining of liver tissues with fibrosis quantification. **J.** Western blot analysis of Collagen I and α-SMA protein levels in liver tissues. Data are presented as mean ± SD ($n = 8$); * $p < 0.05$.

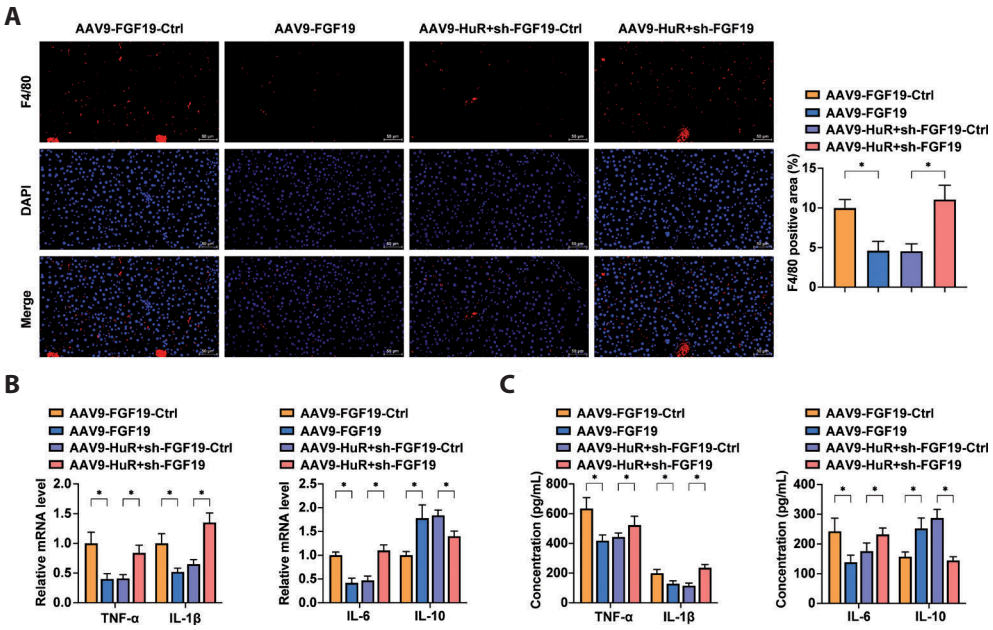

Figure 8. HuR suppresses Kupffer cell activation and hepatic inflammation in NAFLD mice *via* FGF19. **A.** Immunofluorescence staining for F4/80 expression in liver tissues. RT-qPCR analysis (**B**) and ELISA measurement (**C**) of TNF-α, IL-1β, IL-6, and IL-10 mRNA levels in liver tissues. Data are presented as mean ± SD (n = 8); * $p < 0.05$.

effects of HuR overexpression on HFD-induced liver damage, with a significant increase in LW/BW ratio, as well as higher ALT and AST levels (Fig. 7D–F). Moreover, FGF19 knockdown exacerbated lipid accumulation and liver fibrosis, as evidenced by histological analysis, and elevated Collagen I and α-SMA (Fig. 7G–I). Knockdown of FGF19 also reversed the inhibitory effects of HuR on KC activation and inflammation, as shown by increased F4/80, TNF-α, IL-1β, and IL-6, along with decreased IL-10 expression (Fig. 8A–C). Together, these findings indicate that FGF19 mediates the anti-inflammatory and anti-fibrotic actions of HuR in NAFLD, underscoring the therapeutic potential of targeting this pathway.

Discussion

As a quintessential RBP, HuR is ubiquitously expressed across tissues and plays a pivotal role in regulating cell proliferation, stress responses, apoptosis, differentiation, aging, and immune modulation (Srikantan and Gorospe 2012). Prior studies have demonstrated that liver-specific HuR deficiency exacerbates the progression from NAFLD to HCC (Subramanian et al. 2022). However, the role of HuR in regulating KC activation during the transition from NAFLD to inflammation and fibrosis has not been fully elucidated. The absence of HuR specifically in the liver leads to increased fat buildup by affecting fatty acid synthesis and metabolism, while also triggering inflammation under metabolic stress by boosting immune cell infiltration and neutrophil activation (Wang et al. 2022). Our findings provide compelling evidence that HuR expression is downregulated in NAFLD and that HuR mitigates HFD-induced liver inflammation and fibrosis by modulating the pro-inflammatory M1 polarization of KCs.

KCs are critical immune cells in the pathogenesis of NAFLD/NASH, and they represent a central source of inflammatory mediators driving obesity and insulin resistance in NAFLD patients (Tacke 2017; Gao et al. 2022). Under normal conditions, macrophages are tolerant and tend to adopt an M2 phenotype, which is characterized by the production of anti-inflammatory cytokines. However, during the progression of NAFLD, various stimuli, including free fatty acids and lipopolysaccharides, induce the shift of KCs from an M2 to an M1 phenotype. This polarization results in an overproduction of pro-inflammatory cytokines like TNF-α, IL-1β, and IL-6, which subsequently causes chronic inflammation and encourages the progression of NASH. This pathological cascade ultimately results in hepatocyte damage, liver fibrosis, and, in advanced stages, cirrhosis (Liu et al. 2016; Luo et al. 2018; Kumar et al. 2021; Hammerich and Tacke 2023). This study demonstrate that overexpression of HuR *in vivo* significantly ameliorates HFD-induced hepatic injury, steatosis, inflammation, and fibrosis, thereby corroborating previous findings. Notably, our data further indicate that HuR suppresses the activation of pro-inflammatory M1 KCs, providing new insights into the mechanistic regulation of NAFLD progression by HuR.

Mechanistically, HuR exerts its effects by binding to the 3'UTR of FGF19 mRNA, stabilizing its transcript and enhancing its expression. Previous studies have shown that HuR stabilizes numerous target mRNAs, many of which

are involved in pathological processes such as cancer and inflammation (Srikantan and Gorospe 2012). Through bioinformatics prediction, we identified a potential interaction between HuR and FGF19. FGF19 is a key regulator of bile acid metabolism, carbohydrate homeostasis, energy balance, and liver regeneration (Tian et al. 2023). FGF19 levels are significantly reduced in the serum of NASH patients (Jiao et al. 2018), and FGF19/FGF21 analogs have been shown to effectively alleviate hepatic steatosis, steatohepatitis, and liver fibrosis (Tacke et al. 2023). However, the role of FGF19 in KC activation has not been previously explored. After confirming the interaction between HuR and FGF19, we further investigated the role of FGF19 in the development of NAFLD. Consistent with previous findings, we observed that FGF19 expression was significantly downregulated in NAFLD. Notably, upregulation of FGF19 ameliorated liver injury, steatosis, inflammation, and fibrosis in NAFLD, and inhibited M1 KC activation. Moreover, our rescue experiments revealed that knockdown of FGF19 effectively reversed the protective effects of HuR on liver inflammation and fibrosis, as well as its inhibition of KC activation. These results confirm our hypothesis that HuR, by enhancing the stability of FGF19 mRNA, suppresses KC activation and improves the inflammatory and fibrotic responses in NAFLD.

Conclusion

In summary, our data reveal that the interaction between HuR and FGF19 mRNA is a critical molecular mechanism regulating KC activation during NAFLD progression. By enhancing FGF19 mRNA stability, HuR suppresses pro-inflammatory M1 KC activation, thereby mitigating liver injury, steatosis, inflammation, and fibrosis in NAFLD. These findings provide novel insights into the molecular pathways underlying NAFLD and offer potential therapeutic targets for the diagnosis and treatment of this disease.

Funding. The Guangdong Provincial Medical Science and Technology Research Fund Project (No. B2013380). Zhanjiang City Science and Technology Research Project (No. 2019B01096). Zhanjiang City Science and Technology Research Project (No. 2019B01258)

Conflict of interest. The authors have no conflicts of interest to declare.

Availability of data and materials. The datasets used and/or analyzed during the present study are available from the corresponding author on reasonable request.

Ethics approval. All animal experiments were complied with the ARRIVE guidelines and performed in accordance with the National Institutes of Health Guide for the Care and Use of Laboratory Animals. The experiments were approved by the Institutional Animal Care and Use Committee of Central People's Hospital of Zhanjiang (No. B2013380).

Author's contribution. XM and SZ designed the research study and performed the research. XZ and ChH provided help and advice and analyzed the data. XM and SZ wrote the manuscript. SZ reviewed and edited the manuscript. All authors contributed to editorial changes in the manuscript. All authors read and approved the final manuscript.

References

Abdelmalek MF (2021): Nonalcoholic fatty liver disease: another leap forward. Nat. Rev. Gastroenterol. Hepatol. **18,** 85-86 https://doi.org/10.1038/s41575-020-00406-0

Abdelmohsen K, Gorospe M (2010): Posttranscriptional regulation of cancer traits by HuR. Wiley Interdiscip. Rev. RNA **1,** 214-229 https://doi.org/10.1002/wrna.4

Carmona-Hidalgo B, González-Mariscal I, García-Martín A, Prados ME, Ruiz-Pino F, Appendino G, Tena-Sempere M, Muñoz E (2021): Δ9-Tetrahydrocannabinolic acid markedly alleviates liver fibrosis and inflammation in mice. Phytomedicine **81,** 153426 https://doi.org/10.1016/j.phymed.2020.153426

Corley M, Burns MC, Yeo GW (2020): How RNA-binding proteins interact with RNA: Molecules and mechanisms. Mol. Cell. **78,** 9-29 https://doi.org/10.1016/j.molcel.2020.03.011

Cotter TG, Rinella M (2020): Nonalcoholic fatty liver disease 2020: The state of the disease. Gastroenterology **158,** 1851-1864 https://doi.org/10.1053/j.gastro.2020.01.052

Dou L, Shi X, He X, Gao Y (2019): Macrophage phenotype and function in liver disorder. Front. Immunol. **10,** 3112 https://doi.org/10.3389/fimmu.2019.03112

Friedman SL, Neuschwander-Tetri BA, Rinella M, Sanyal AJ (2018): Mechanisms of NAFLD development and therapeutic strategies. Nat. Med. **24,** 908-922 https://doi.org/10.1038/s41591-018-0104-9

Gao H, Jin Z, Bandyopadhyay G, Rocha E, Cunha K, Liu X, Zhao H, Zhang D, Jouihan H, Pourshahian S, et al. (2022): MiR-690 treatment causes decreased fibrosis and steatosis and restores specific Kupffer cell functions in NASH. Cell Metab. **34,** 978-990.e4 https://doi.org/10.1016/j.cmet.2022.05.008

Grammatikakis I, Abdelmohsen K, Gorospe M (2017): Posttranslational control of HuR function. Wiley Interdiscip. Rev. RNA **8,** 10.1002 https://doi.org/10.1002/wrna.1372

Hammerich L, Tacke F (2023): Hepatic inflammatory responses in liver fibrosis. Nat. Rev. Gastroenterol. Hepatol. **20,** 633-646 https://doi.org/10.1038/s41575-023-00807-x

Jiao N, Baker SS, Chapa-Rodriguez A, Liu W, Nugent CA, Tsompana M, Mastrandrea L, Buck MJ, Baker RD, Genco RJ, et al. (2018): Suppressed hepatic bile acid signalling despite elevated

production of primary and secondary bile acids in NAFLD. Gut **67,** 1881-1891
https://doi.org/10.1136/gutjnl-2017-314307

Kazankov K, Jørgensen SMD, Thomsen KL, Møller HJ, Vilstrup H, George J, Schuppan D, Grønbæk H (2019): The role of macrophages in nonalcoholic fatty liver disease and nonalcoholic steatohepatitis. Nat. Rev. Gastroenterol. Hepatol. **16,** 145-159
https://doi.org/10.1038/s41575-018-0082-x

Kleiner DE, Brunt EM, Van Natta M, Behling C, Contos MJ, Cummings OW, Ferrell LD, Liu YC, Torbenson MS, Unalp-Arida A, et al. (2005): Design and validation of a histological scoring system for nonalcoholic fatty liver disease. Hepatology **41,** 1313-1321
https://doi.org/10.1002/hep.20701

Kolios G, Valatas V, Kouroumalis E (2006): Role of Kupffer cells in the pathogenesis of liver disease. World J. Gastroenterol. **12,** 7413-7420
https://doi.org/10.3748/wjg.v12.i46.7413

Kumar S, Duan Q, Wu R, Harris EN, Su Q (2021): Pathophysiological communication between hepatocytes and non-parenchymal cells in liver injury from NAFLD to liver fibrosis. Adv. Drug Deliv. Rev. **176,** 113869
https://doi.org/10.1016/j.addr.2021.113869

Lazarus JV, Mark HE, Anstee QM, Arab JP, Batterham RL, Castera L, Cortez-Pinto H, Crespo J, Cusi K, Dirac MA, et al. (2022): Advancing the global public health agenda for NAFLD: a consensus statement. Nat. Rev. Gastroenterol. Hepatol. **19,** 60-78

Li P, He K, Li J, Liu Z, Gong J (2017): The role of Kupffer cells in hepatic diseases. Mol. Immunol. **85,** 222-229
https://doi.org/10.1016/j.molimm.2017.02.018

Lin Z, Yang P, Hu Y, Xu H, Duan J, He F, Dou K, Wang L (2023): RING finger protein 13 protects against nonalcoholic steatohepatitis by targeting STING-relayed signaling pathways. Nat. Commun. **14,** 6635
https://doi.org/10.1038/s41467-023-42420-1

Liu X, Yu L, Hassan W, Sun L, Zhang L, Jiang Z (2016): The duality of Kupffer cell responses in liver metabolic states. Curr. Mol. Med. **16,** 809-819
https://doi.org/10.2174/1566524016666161031143724

Loomba R, Friedman SL, Shulman GI (2021): Mechanisms and disease consequences of nonalcoholic fatty liver disease. Cell **184,** 2537-2564
https://doi.org/10.1016/j.cell.2021.04.015

Luo X, Li H, Ma L, Zhou J, Guo X, Woo SL, Pei Y, Knight LR, Deveau M, Chen Y, et al. (2018): ,Expression of STING is increased in liver tissues from patients with NAFLD and promotes macrophage-mediated hepatic inflammation and fibrosis in mice. Gastroenterology **155,** 1971-1984e4
https://doi.org/10.1053/j.gastro.2018.09.010

Makri E, Goulas A, Polyzos SA (2021): Epidemiology, pathogenesis, diagnosis and emerging treatment of nonalcoholic fatty liver disease. Arch. Med. Res. **52,** 25-37
https://doi.org/10.1016/j.arcmed.2020.11.010

Mosser DM, Edwards JP (2008): Exploring the full spectrum of macrophage activation. Nat. Rev. Immunol. **8,** 958-969
https://doi.org/10.1038/nri2448

Park SJ, Garcia Diaz J, Um E, Hahn YS (2023): Major roles of kupffer cells and macrophages in NAFLD development. Front. Endocrinol. (Lausanne) **14,** 1150118
https://doi.org/10.3389/fendo.2023.1150118

Paternostro R, Trauner M (2022): Current treatment of nonalcoholic fatty liver disease. J. Intern. Med. **292,** 190-204
https://doi.org/10.1111/joim.13531

Powell EE, Wong VW, Rinella M (2021): Non-alcoholic fatty liver disease. Lancet **397,** 2212-2224
https://doi.org/10.1016/S0140-6736(20)32511-3

Rong L, Zou J, Ran W, Qi X, Chen Y, Cui H, Guo J (2022): Advancements in the treatment of non-alcoholic fatty liver disease (NAFLD). Front. Endocrinol. (Lausanne) **13,** 1087260
https://doi.org/10.3389/fendo.2022.1087260

Schultz CW, Preet R, Dhir T, Dixon DA, Brody JR (2020): Understanding and targeting the disease-related RNA binding protein human antigen R (HuR). Wiley Interdiscip. Rev. RNA **11,** e1581
https://doi.org/10.1002/wrna.1581

Srikantan S, Gorospe M (2012): HuR function in disease. Front. Biosci. (Landmark Ed.) **17,** 189-205
https://doi.org/10.2741/3921

Subramanian P, Gargani S, Palladini A, Chatzimike M, Grzybek M, Peitzsch M, Papanastasiou AD, Pyrina I, Ntafis V, Gercken B, et al. (2022): The RNA binding protein human antigen R is a gatekeeper of liver homeostasis. Hepatology **75,** 881-897
https://doi.org/10.1002/hep.32153

Tacke F (2017): Targeting hepatic macrophages to treat liver diseases. J. Hepatol. **66,** 1300-1312
https://doi.org/10.1016/j.jhep.2017.02.026

Tacke F, Puengel T, Loomba R, Friedman SL (2023): An integrated view of anti-inflammatory and antifibrotic targets for the treatment of NASH. J. Hepatol. **79,** 552-566
https://doi.org/10.1016/j.jhep.2023.03.038

Tian H, Zhang S, Liu Y, Wu Y, Zhang D (2023): Fibroblast growth factors for nonalcoholic fatty liver disease: Opportunities and challenges. Int. J. Mol. Sci. **24,** 4583
https://doi.org/10.3390/ijms24054583

Tian L, Chen J, Yang M, Chen L, Qiu J, Jiang Y, Tan X, Qian Q, Liang X, Dou X (2024): Xiezhuo Tiaozhi formula inhibits macrophage pyroptosis in the non-alcoholic fatty liver disease by targeting the SIRT1 pathway. Phytomedicine **131,** 155776
https://doi.org/10.1016/j.phymed.2024.155776

Tian M, Wang J, Liu S, Li X, Li J, Yang J, Zhang C, Zhang W (2021): Hepatic HuR protects against the pathogenesis of non-alcoholic fatty liver disease by targeting PTEN. Cell. Death Dis. **12,** 236
https://doi.org/10.1038/s41419-021-03514-0

Tran S, Baba I, Poupel L, Dussaud S, Moreau M, Gélineau A, Marcelin G, Magréau-Davy E, Ouhachi M, Lesnik P, et al. (2020): Impaired Kupffer cell self-renewal alters the liver response to lipid overload during non-alcoholic steatohepatitis. Immunity **53,** 627-640.e5
https://doi.org/10.1016/j.immuni.2020.06.003

Wan J, Benkdane M, Teixeira-Clerc F, Bonnafous S, Louvet A, Lafdil F, Pecker F, Tran A, Gual P, Mallat A, et al. (2014): M2 Kupffer cells promote M1 Kupffer cell apoptosis: a protective mechanism against alcoholic and nonalcoholic fatty liver disease. Hepatology **59,** 130-142
https://doi.org/10.1002/hep.26607

Wang Q, Ou Y, Hu G, Wen C, Yue S, Chen C, Xu L, Xie J, Dai H, Xiao H, et al. (2020): Naringenin attenuates non-alcoholic fatty liver disease by down-regulating the NLRP3/NF-κB pathway in mice. Br. J. Pharmacol. **177,** 1806-1821 https://doi.org/10.1111/bph.14938

Wang Y, Tai YL, Way G, Zeng J, Zhao D, Su L, Jiang X, Jackson KG, Wang X, Gurley EC (2022): RNA binding protein HuR protects against NAFLD by suppressing long noncoding RNA H19 expression. Cell Biosci. **12,** 172 https://doi.org/10.1186/s13578-022-00910-7

Wei D, Tian X, Zhu L, Wang H, Sun C (2023): USP14 governs CYP2E1 to promote nonalcoholic fatty liver disease through deubiquitination and stabilization of HSP90AA1. Cell Death Dis. **14,** 566 https://doi.org/10.1038/s41419-023-06091-6

Xu J, Liu X, Wu S, Zhang D, Liu X, Xia P, Ling J, Zheng K, Xu M, Shen Y, et al. (2023): RNA-binding proteins in metabolic-associated fatty liver disease (MAFLD): From mechanism to therapy. Biosci. Trends **17,** 21-37 https://doi.org/10.5582/bst.2022.01473

Xu X, Poulsen KL, Wu L, Liu S, Miyata T, Song Q, Wei Q, Zhao C, Lin C, Yang J (2022): Targeted therapeutics and novel signaling pathways in non-alcohol-associated fatty liver/steatohepatitis (NAFL/NASH). Signal. Transduct. Target Ther. **7,** 287 https://doi.org/10.1038/s41392-022-01119-3

Zhang Z, Yuan Y, Hu L, Tang J, Meng Z, Dai L, Gao Y, Ma S, Wang X, Yuan Y, et al. (2023): ANGPTL8 accelerates liver fibrosis mediated by HFD-induced inflammatory activity via LILRB2/ERK signaling pathways. J. Adv. Res. **47,** 41-56 https://doi.org/10.1016/j.jare.2022.08.006

Zhang Z, Zong C, Jiang M, Hu H, Cheng X, Ni J, Yi X, Jiang B, Tian F, Chang MW, et al. (2020): Hepatic HuR modulates lipid homeostasis in response to high-fat diet. Nat. Commun. **11,** 3067 https://doi.org/10.1038/s41467-020-16918-x

Received: January 21, 2025
Final version accepted: May 5, 2025